Concentration Dependence of Water Dynamics in Poly(Ethylene Oxide)/Water Solutions from Molecular Dynamics Simulations

Oleg Borodin,* Dmitry Bedrov, and Grant D. Smith

Department of Materials Science and Engineering and Department of Chemical and Fuels Engineering University of Utah, 122 S. Central Campus Drive Rm. 304, Salt Lake City, Utah 84112

Received: July 31, 2001; In Final Form: January 7, 2002

We have performed molecular dynamics simulations of aqueous solutions of poly(ethylene oxide) (PEO) in order to investigate the influence of the polymer on water dynamics. Simulations were performed on 12 repeat unit CH_3-capped PEO chains (530 Da) at 318 K covering a composition range (polymer weight fraction) from 0.17 to 1.0. The simulations employed an ab initio quantum-chemistry-based PEO/water and PEO/PEO force field together with the TIP4P (four-point transferable intermolecular potential) water model. Water translational and rotational diffusion were found to slow monotonically, whereas water−water and water-ether hydrogen bond lifetimes increased with increasing polymer concentration. The slowing of water dynamics in PEO/water solutions was associated with PEO−water interactions that are moderated in concentrated solutions by the formation of water clusters. Water translational motion could be ascribed to a combination of free water (water not involved with PEO hydration) that exhibited bulklike water dynamics and bound (hydrating water) whose motion was strongly correlated with that of the PEO molecule. Water rotational motion was found to be strongly correlated with translation motion and exhibited increasing anisotropy with increasing PEO concentration indicative of preferred rotation of the water molecules around their dipole moment vector. At high PEO concentration, water and ether oxygen atoms exhibited well pronounced subdiffusive behavior occurring on a picosecond time scale that disappears upon dilution. The characteristic length scale for the water subdiffusive behavior associated with water caging correlates well with nearest-neighbor ether oxygen−ether oxygen distance.

I. Introduction

Applications of poly(ethylene oxide) (PEO) in aqueous solutions include protein crystallization,[1−3] modification of surfaces for biocompatibility,[4,5] control of particle aggregation in solution,[6,7] modification of natural and artificial membranes,[8,9] and aqueous biphasic separations.[10] Because of the widespread importance of PEO in aqueous solutions, we[11−15] and other groups[16−20] have conducted molecular dynamics (MD) simulation studies in order to gain atomistic level insight into the thermodynamics and dynamics of PEO and its oligomers in aqueous solutions. This paper is the third in a series dealing with the dynamic properties of PEO/water solutions from MD simulations. In the previous paper of this issue,[21] we studied water dynamics in PEO/water solutions as a function of temperature by MD simulations and quasielastic neutron scattering (QNS) experiments at a single composition ($w_p = 0.52$). Water rotational diffusion was found to be highly anisotropic at 298 K, with anisotropy gradually decreasing with increasing temperature. Good agreement for the water self-diffusion coefficient from MD simulations and QNS experiments was found,[21] further validating the quantum chemistry based potential used in the MD simulations. We also studied[22] the composition dependence of polymer dynamics which were found to be strongly influenced by water. Specifically, water slows the rate of conformational transitions in PEO compared to the melt, an effect that sets in rapidly with initial dilution but saturates at polymer weight fraction $w_P \approx 0.5$. At this composition, PEO−water hydrogen bonding is nearly saturated, and the first PEO−water hydration shell is largely formed.[23] Water also was found to initially lead to an increase, and then to a dramatic decrease in solution viscosity as well as polymer relaxation times on all length scales, with the effect later confirmed by viscosity and QNS measurements.[24] In this contribution, we consider in detail rotational and translational dynamics of water in PEO/water solutions as a function of concentration.

II. Molecular Dynamics Simulation Methodology

A quantum-chemistry-based force field for PEO/PEO[25] and PEO/water interactions[11] together with the transferable intermolecular four-point potential (TIP4P) model for water[26] were used in our simulations. MD simulations were performed on aqueous solutions of 12 repeat unit PEO chains of the structure $H-(CH_2-O-CH_2)_{12}-H$ for compositions $w_p = 0.17$, 0.35, 0.52, 0.65, 0.78, 0.90, and 0.999 at 318 K. The composition $w_P = 0.999$ corresponds to a system of 32 PEO chains with a single water molecule. For this composition, two independent systems were simulated in order to improve statistics. For other compositions, the simulation box was comprised of approximately 4000 atoms with 8−32 PEO chains depending on composition. The Ewald summation method[27] was used to calculate long-range Coulomb interactions. Bond lengths were constrained using the Shake algorithm.[28] A 10.0 Å truncation radius was used for dispersion interactions. Simulations of 0.5−2.0 ns were performed in an NPT ensemble using the velocity Verlet algorithm[27] to establish solution densities at atmospheric pressure. Those densities were used in subsequent NVT simulations employing a multiple time step reversible reference system

* To whom correspondence should be addressed.

10.1021/jp012949t CCC: $22.00
Published on Web 04/30/2002

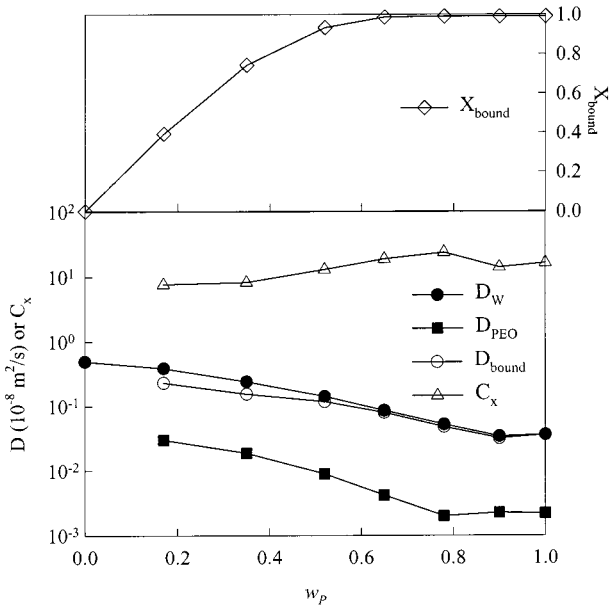

Figure 1. Water and PEO self-diffusion coefficient for PEO/water solutions. Also shown are the diffusion coefficient of bound water and the C_x parameter from eq 1.

propagator algorithm[29,30] with a time step of 0.7 fs for bonding, bending, and torsional motions, with a 1.4 fs time step for nonbonded interactions within a 6.5 Å sphere, and with a 2.8 fs time step for nonbonded interactions between 6.5 and 10.0 Å and the reciprocal space part of the Ewald summation. Production runs were 20−50 ns.

MD simulations of PEO/water solutions at $w_P = 0.9$ with water−water electrostatic interactions turned off were also performed in order to investigate the effect of water clustering on water and polymer dynamics. These simulations were performed in NVT ensemble for 3 ns at the same density as in the system with all interactions turned on.

III. Water Self-Diffusion

The self-diffusion coefficient of water is shown in Figure 1 as a function of solution composition. Also shown is the self-diffusion coefficient for PEO, whose behavior as a function of solution composition is discussed in a previous paper.[22] The self-diffusion coefficient of water exhibits a monotonic decrease with increasing polymer concentration with saturation at $w_P = 0.9$. By contrast, in simulations of 1,2-dimethoxyethane (DME)/water solutions,[13] we found that water diffusion exhibited a minimum at $w_{DME} \approx 0.5-0.75$ which was subsequently confirmed experimentally.[15] Similarly, pulsed-field gradient spin−echo NMR investigations[31] of oligomers of ethylene glycol [HO−(CH_2−CH_2−O)$_n$-H, $n = 1-5$] in water revealed that the water self-diffusion decreases with increasing oligomer concentration until a composition corresponding roughly to one water molecule per EO monomer. Further increase in oligo(ethylene glycol) concentration did not lead to additional significant decrease in the water or oligo(ethylene glycol) self-diffusion coefficients. In the case of DME/water solutions, we were able to accurately represent the composition dependence of the self-diffusion coefficient of water using the expression:[13]

$$D_w = (1 - X_{bound})D_o + X_{bound}C_x D_{PEO} \quad (1)$$

where D_w is the composition dependent self-diffusion coefficient of water, D_o is the self-diffusion coefficient of free water assumed to be equal to that of pure water, D_{PEO} is the composition dependent self-diffusion coefficient of the ether, X_{bound} is the fraction of water considered to be bound to an ether molecule, and C_x is an unknown proportionality constant. For DME/water solutions, we obtained D_o, D_{PEO}, and X_{bound} from simulations, leaving C_x as the only adjustable parameter to reproduce D_w as a function of composition.[13] X_{bound} was determined by assuming that all water molecules within the first hydration shell of an ether molecule, defined based upon intermolecular pair distribution functions as all water molecules whose oxygen atom lies with 3.7 Å of an ether oxygen atom or 4.2 Å of an ether carbon atom, are bound to the ether. We found that eq 1 provided a good description of D_{water} in DME solutions for $C_x = 1.4$ independent of composition. The supposition behind eq 1, which is supported by the good representation of the water self-diffusion it provides, is that the translational motion of water molecules in the first hydration shell of the ether is strongly correlated with motion of the ether, whereas those water molecules not directly involved with ether hydration exhibit bulk-water-like dynamics.

Figure 1 shows the fraction of bound water molecules in PEO/water solutions as a function of composition as well as the values of C_x for each composition required to reproduce D_w using eq 1. Unlike DME/water solutions, C_x shows some composition dependence. However, the self-diffusion coefficient of bound water, given by (C_xD_{PEO}), is approximately 1 order of magnitude greater than that of PEO over the entire range of composition, indicating that the translational motion of bound water is strongly correlated with ether motion in PEO/water as well as DME/water solutions. A value of C_x much greater than unity indicates that unlike DME solutions, where motion of bound water is correlated with the center of mass motion of the ether (i.e., C_x is on the order of unity), bound water diffusion in solutions of the much larger PEO molecule appears to be correlated with smaller length scale motions of the polymer. Finally, the strong correlation of bound water motion with the motion of the polymer accounts for the continued monotonic decrease in water self-diffusion coefficient in the more concentrated PEO solutions for $w_P < 0.9$ because PEO motion is much slower than water diffusion, in contrast to smaller ethers such as DME where water and ether diffusion are comparable, and water diffusion exhibits a minimum at $w_{DME} \approx 0.5-0.75$.

IV. Rotational Water Dynamics

We investigated the rotational motion of water by examining the motion of the three vectors shown in Figure 2: a vector (**HH**) connecting the hydrogen atoms, a vector directed along the bisector of the H−O−H bend, corresponding to the direction of the water dipole moment (μ), and a vector perpendicular to the plane of a water molecule ($\perp$). These vectors correspond to the principal axes of the water molecule. $P_1(t)$ and $P_2(t)$ autocorrelation functions for orientational relaxation of the vectors are given by

$$P_1(t) = \langle[\mathbf{e}(t)\cdot\mathbf{e}(0)]\rangle \quad (2)$$

$$P_2(t) = 0.5[3\langle[\mathbf{e}(t)\cdot\mathbf{e}(0)]^2\rangle - 1] \quad (3)$$

where $\mathbf{e}(t)$ is a unit vector in the direction of the **HH**, μ, or $\perp$ vector, t is time, and $\langle\rangle$ denotes the ensemble average over all such vectors.

A. Rotational Relaxation Times. Decay of the $P_1(t)$ and $P_2(t)$ autocorrelation functions to 0.01 obtained from MD simulations was approximated by a Kohlrausch−Williams−Watts (KWW) expression given by

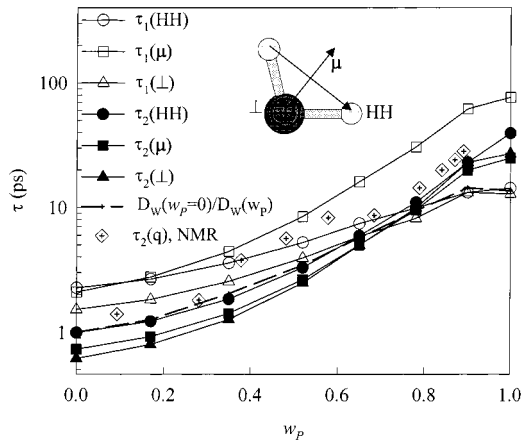

Figure 2. Rotational (τ_1, τ_2) and relaxation times for water in PEO/water solutions from MD simulations. Scaled rotational relaxation times $\tau_2(q)$ from NMR experiments are also shown.

$$P_{\mathrm{KWW}}(t) = \exp[-(t/\tau)^{\beta}] \tag{4}$$

Rotational autocorrelation times τ_1 and τ_2 were calculated as time integrals of the KWW fits to $P_1(t)$ and $P_2(t)$ and are shown in Figure 2 as a function of polymer concentration. All rotational relaxation times increase with increasing polymer concentration demonstrating slowing down of water rotation. The concentration dependence of τ_2 from our MD simulations compares well with the τ_2 for water rotation obtained from spin−spin and spin−lattice relaxation NMR measurements[32] on PEO/^2H_2O (MW = 6000) at room temperature, also shown in Figure 2. As these experiments were performed at 298 K on PEO/^2H_2O solutions while our MD simulations were performed at 318 K on PEO/H_2O, the experimental values in Figure 2 were scaled by at factor 2.6 in order to take into account the difference between water rotational relaxation times at 318 and 298 K as well as the difference of rotational relaxation of H_2O and ^2H_2O.[33]

B. Anisotropy of Water Rotation. Although the τ_2 relaxation times have similar concentration dependence for the **HH**, μ, and $\perp$ vectors, the increase of $\tau_1(\mu)$ with increasing PEO concentration is much more dramatic than that of τ_1(**HH**) and $\tau_1(\perp)$. Significant differences between $\tau_1(\mu)$ and τ_1(**HH**) or $\tau_1(\perp)$ at high PEO concentration is indicative of anisotropy in water rotational motion. The ratios τ(**HH**)/$\tau(\mu)$ and τ(**HH**)/$\tau(\perp)$, shown in Figure 3, are a measure of this anisotropy. Each of these ratios is close to unity for pure water, indicating that water rotation in pure water at 318 K is approximately isotropic in agreement with the previous MD simulation studies at 298 K.[34] Addition of PEO leads to a monotonic decrease of τ_1(**HH**)/$\tau_1(\mu)$ indicative of much faster (up to an order of magnitude) rotation of the **HH** vector compared to the μ vector in concentrated solutions. The ratio of τ(**HH**)/$\tau(\perp)$ on the other hand stays close to unity for all solution compositions. In addition, although τ_1(**HH**)/$\tau_1(\mu)$ drops much below unity for concentrated PEO solutions, the ratio τ_2(**HH**)/$\tau_2(\mu)$ does not. The reasons for this apparent difference become clear when the ratio of the τ_1 and τ_2 autocorrelation times, shown in Figure 4, is examined. This ratio is expected to be three for completely isotropic vector rotation, much larger than three for vector rotation restricted to the surface of a cone and much smaller than three for vector rotation in a plane. The ratios τ_1(**HH**)/τ_2(**HH**) and $\tau_1(\perp)/\tau_2(\perp)$ drop significantly below three as the PEO concentration increases, indicative of preferential water rotation in a plane including both the **HH** and $\perp$ vectors. The only plane in which such motion is possible is the plane perpendicular to the μ vector. Thus, water rotation in the plane perpendicular to μ is much faster than the rotation of the μ vector at high PEO concentrations. This picture is consistent with the τ_1(**HH**)/$\tau_1(\mu)$ being much smaller than one, whereas the τ_2(**HH**)/$\tau_2(\mu)$ ratio is still close to unity.

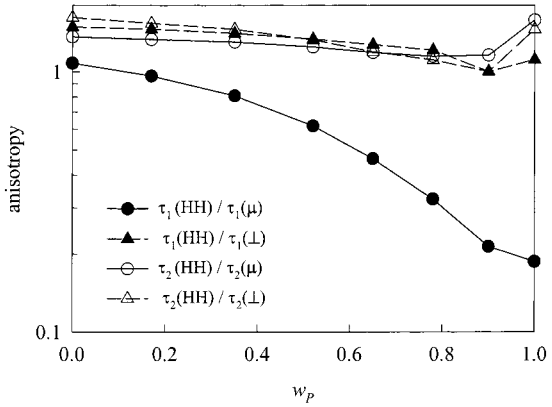

Figure 3. Anisotropy of water rotational relaxation as a function of PEO concentrations.

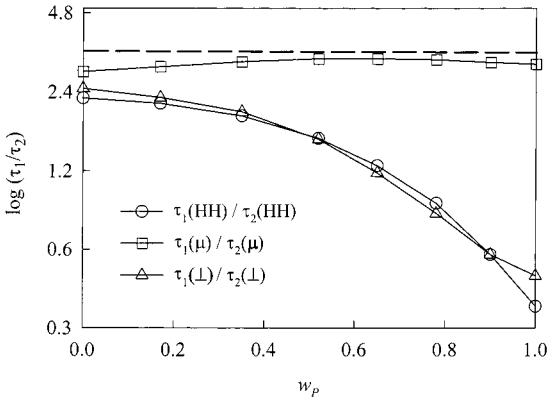

Figure 4. Ratio of τ_1/τ_2 rotational relaxation times as a function of PEO concentrations.

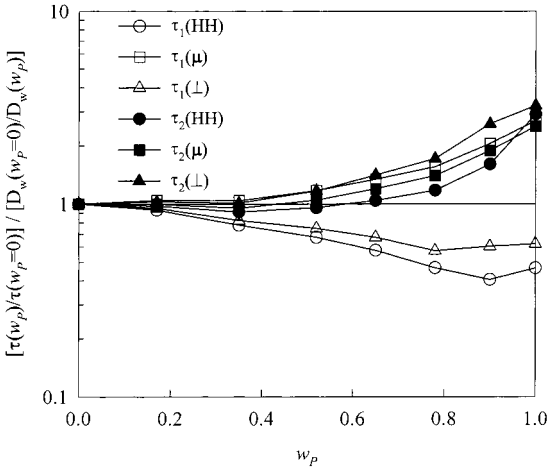

Figure 5. Ratio of rotational and translational relaxation times normalized to those of pure water as a function of PEO concentrations.

C. Coupling of Rotational and Translational Motion. To investigate the coupling of translational and rotational diffusion of water, we plotted the ratio of the rotational relaxation times to the translational relaxation time of water, given as $1/D_w$, normalized to values for pure water, as shown in Figure 5. All ratios are close to unity, with τ_2(HH) being the closest. This indicates that a picture of water rotational dynamics in PEO/water solutions analogous to that provided above for translational motion may be applicable: water not involved in the hydration

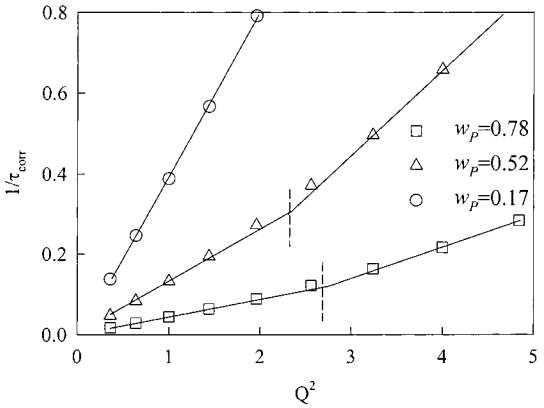

Figure 6. Inverse translational correlation time of water in PEO/water solutions. Vertical lines indicate the position of the change of slope.

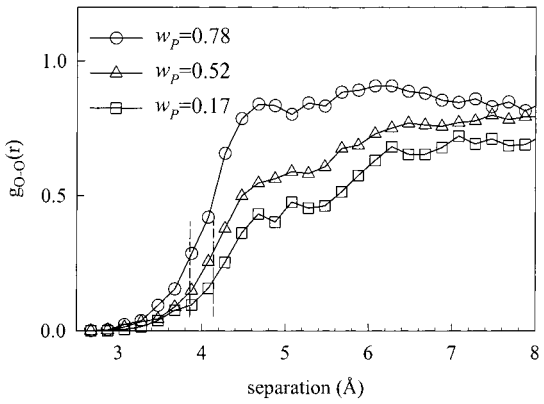

Figure 7. Ether oxygen−ether oxygen intermolecular radial distribution functions for PEO/water solutions. Dashed lines indicate the expected caging size from the $\Gamma(Q^2)$ analysis.

of PEO manifests bulk water-like dynamics, whereas the dynamics of bound water are correlated with the polymer dynamics.

V. Caging of Water by PEO

The intermediate incoherent structure factor, given by

$$I_{\mathrm{inc}}(Q,t) = \left\langle \frac{\sin(r_i(t)Q)}{r_i(t)Q} \right\rangle \tag{5}$$

where $r_i(t)$ is the displacement of center of mass of water molecule i after time t, Q is the magnitude of the momentum transfer vector, and $\langle\ \rangle$ denotes an average over all time origins and water molecules. If the displacements of water center of mass are Gaussian distributed, the water center of mass incoherent structure factor is given by

$$I_{\mathrm{cm}}(Q,t) = \exp[-Q^2\langle r^2(t)\rangle/6] \tag{6}$$

where $\langle r^2(t)\rangle$ is the mean-square displacement of water center of mass after time t. Furthermore, assigning $D(t) = \langle r^2(t)\rangle/6t$, we obtain

$$I_{\mathrm{cm}}(Q,t) = \exp[-Q^2D(t)t] \tag{7}$$

where $D(t)$ is the instantaneous diffusion coefficient. Even when the displacement distribution is not Gaussian, an apparent diffusion coefficient can be determined from the relationship

$$\Gamma(Q) = Q^2D_{\mathrm{app}}(t) = -\ln[I_{\mathrm{cm}}(Q/t)]/t = 1/\tau_{\mathrm{corr}} \tag{8}$$

where $\Gamma(Q)$ is the line width of the translational component and is equal to the inverse translational correlation time ($1/\tau_{\mathrm{corr}}$). The translational correlation time (τ_{corr}) is defined as a time integral of $I_{\mathrm{cm}}(Q,t)$ from zero to infinity. In accord with Sciortino et al.[35] and our previous findings,[21] we found that the decay of $I_{\mathrm{cm}}(Q,t)$ could be nicely approximated by a modified KWW expression

$$I_{\mathrm{cm}}(Q,t) = [1 - A(Q)]\exp[-(t/\tau_{\mathrm{s}})^2] + A(Q)\exp[-(t/\tau_{\mathrm{long}})^{\beta}] \tag{9}$$

The first term in eq 9 describes the processes on the fast time scale, whereas the stretched exponential term describes the slow decay also called α correlation. Inverse translational relaxation times were calculated as time integrals from zero to infinity of the modified KWW fits (eq 9) to $I_{\mathrm{cm}}(Q,t)$. Figure 6 is a plot of $1/\tau_{\mathrm{corr}}$ as function of Q^2 for three solution compositions. If water motion is Gaussian, then the inverse translational correlation time ($1/\tau_{\mathrm{corr}}$; eq 8) would scale proportionally to Q^2 resulting in a straight line in Figure 6. This scaling clearly does not hold for $w_{\mathrm{P}} > 0.52$ as Figure 6 shows that two straight lines are necessary in order to describe the Q^2 dependence of $1/\tau_{\mathrm{corr}}$. This indicates the existence of two water diffusional regimes in PEO/water solutions at $w_{\mathrm{P}} \geq 0.52$: one at large Q values with a high diffusion coefficient and the other at small Q values with a smaller diffusion coefficient. The crossover between these two regimes occurs at $Q = 1.5$ and 1.7 Å^{-1} for $w_{\mathrm{P}} = 0.52$ and 0.78, respectively. In QNS experiments on PEO/water solutions at 303 K, Crupi et al.[36,37] found a similar behavior of water; that is, the translational half-width at half-maximum (analogous to $1/\tau_{\mathrm{corr}}$) plotted vs Q^2 had a clear change of the slope at Q around 1.15 and 0.9 Å^{-1} for $w_{\mathrm{P}} = 0.7$ and 0.53, respectively. This change of the slope was attributed to water caging by PEO chains. Analogously, a change in the slope of ($1/\tau_{\mathrm{corr}(Q)}$) vs Q^2 around $Q = 2\pi/L$, where L is the caging distance, is expected when caging of water motion occurs. At 318 K for $w_{\mathrm{P}} = 0.52$ and 0.78, ($1/\tau_{\mathrm{corr}(Q)}$) clearly exhibits a change of the slope at $Q = 1.5$ and 1.7 Å^{-1}, respectively, whereas for $w_{\mathrm{P}} = 0.17$, the change of the slope is unnoticeable. No break in the slope is seen in pure water (not shown here). The change of the slope shifts to larger Q with increasing polymer concentration, consistent with the caging of water in smaller volumes for higher polymer concentrations.

The intermolecular ether oxygen−ether oxygen radial distribution function (RDF), shown in Figure 7, is a natural candidate for monitoring size of the PEO cage. If the caging picture is correct, we would expect the onset of closest oxygen−oxygen correlations at distances close to L, namely, 4.2 and 3.7 Å for $w_{\mathrm{P}} = 0.52$ and 0.78, respectively, shown by vertical lines in Figure 7. For $w_{\mathrm{P}} = 0.52$ and 0.78, the cage size from the change in slope of $1/\tau_{\mathrm{corr}}$ is in reasonable agreement with the cage size expected from the ether oxygen-ether oxygen intermolecular RDF. At $w_{\mathrm{P}} = 0.17$ the lack of caging seen in Figure 6 is consistent with the majority of water being "free", i.e., unbound water as shown in Figure 1 and therefore not confined by PEO chains. We may conclude that the caging picture makes sense only in concentrated PEO/water solutions.

To obtain better understanding of dynamic water caging complementing the spatial caging picture obtained from Figures 6 and 7, we investigate the caging effect from a point of view of atomic mean-square displacements $\langle r^2\rangle$. We envision that the caging of water molecules by PEO would lead to a two-step diffusion process. In the first step, water would move within

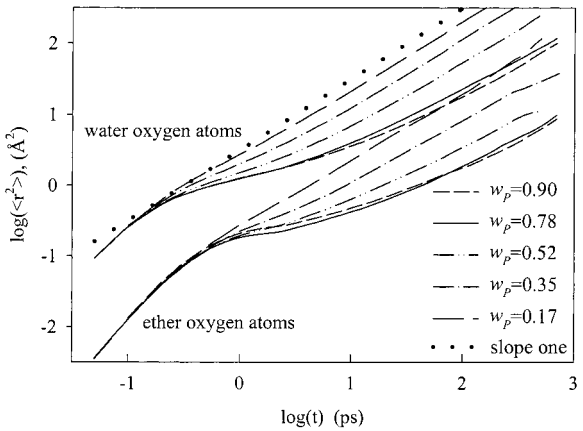

Figure 8. Mean-square displacements of water and PEO oxygen atoms for PEO/water solutions.

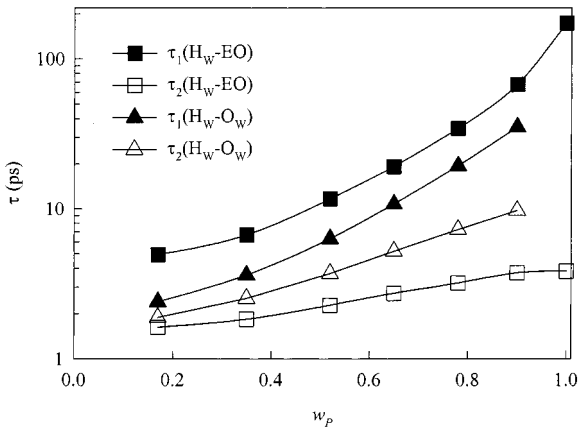

Figure 9. Residence times τ_1 and τ_2 for H_W-EO and H_W-O_W hydrogen bonds.

the cage for some residence time with the diffusion coefficient corresponding to the slope at high Q values in Figure 6. In the second step, water would exhibit a free Fickian diffusion with the diffusion coefficient corresponding to the slope at low Q values in Figure 6. A log−log plot of $\langle r^2 \rangle$ vs time for the oxygen atoms of water and PEO shown in Figure 8 allows one to distinguish between various diffusion regimes. A slope of two is always observed for very short times and corresponds to the ballistic regime, whereas a slope of one is characteristic of a well developed Fickian diffusion regime and is observed at long times. For some systems, a slope of less than one (subdiffusive behavior) is also observed indicative of segment or molecule caging. For concentrated PEO/water solutions, a slope much less than one is clearly seen in Figure 8 for both water and PEO oxygen atom mean square displacement on a picosecond time scale suggesting strong caging of water and domination of PEO motion by conformational transitions on this time scale. Indeed, caging of ether oxygen atoms on a picosecond time scale is consistent with the average time of conformational transitions being about 20 ps.[22] Dilution of PEO/water solutions lessens the subdiffusive behavior (dynamic caging) of water, with the effect completely disappearing at $w_P = 0.17$ where the majority of the water is free (see Figure 1). The subdiffusive character of the polymer motion is also lessened by dilution, indicative of a change in diffusion mechanism in polymer motion from conformational transitions in pure melt to the polymer represented by a particle with a hydrodynamics radius of a polymer coil diffusing in water for dilute PEO/water solutions.[38]

VI. Ether Oxygen−Water and Water−Water Hydrogen Bond Lifetimes

The water−ether oxygen and water−water hydrogen bond mean residence times $\tau(H_w-EO)$ and $\tau(H_w-O_w)$, respectively, are a measure of the lifetime of the PEO−water and water−water hydrogen bonds. We employ two definitions of residence times. In the first definition, the total residence time distribution function is defined by

$$R_1(t) = \langle H(t)\, H(0) \rangle \tag{10}$$

where $H(t) = 1$ if a hydrogen bond exists at time t and zero otherwise and $\langle\rangle$ denotes ensemble average over all possible hydrogen bonds normalized by the average number of hydrogen bonds. In the second definition, the residence time $R_2(t)$ was calculated as an ensemble average of the probability of a hydrogen bond lasting for a duration t. Integrals from zero to infinity of $R_1(t)$ and $R_2(t)$ yield τ_1 and τ_2 respectively and are shown in Figure 9. All residence times (τ_1 and τ_2) increase with increasing PEO concentration, and the τ_1 values are always significantly larger than the τ_2 values because of water molecules reforming hydrogen bonds with PEO oxygen atoms or water molecules. The monotonic increase in PEO−water and water−water bond lifetimes coincides well with monotonic increase in translational and rotational relaxation times with increasing PEO concentration.

The water−water hydrogen bonds are longer lived than the water−ether oxygen hydrogen bonds for all PEO compositions, as $\tau_2(H_w-O_w)$ are always larger than $\tau_2(H_w-EO)$ with the effect being more pronounced at high PEO concentrations. However, the opposite trend is seen for the total hydrogen bond times, where $\tau_1(H_w-O_w)$ is always less than $\tau_1(H_w-EO)$. The different behavior of the τ_1 and τ_2 residence times can be reconciled by a fact that water translational motion is faster than PEO translational motion (Figure 1). Therefore, the probability of water reforming a hydrogen bond with a previously bonded water is less than that for water to reform a hydrogen bond with a previously bonded ether oxygen simply because the water neighbors change more rapidly. Finally, we note that the mean water−ether hydrogen bond lifetime based upon the first exit criterion is less than 10 ps for dilute solutions, which is much shorter than the 250 ps obtained by Tasaki using unvalidated PEO-water force field.[19]

VII. Effect of Water Clustering on Water Dynamics

For concentrated solutions (e.g., $w_P \geq 0.5$), formation of water clusters[23] greatly reduces the number of water−PEO contacts (and hence hydrogen bonds) compared to the number expected for random mixing. Here, we wish to investigate the influence of nonideal mixing on water dynamics in relatively concentrated PEO/water solutions. For this purpose, we performed MD simulations of a PEO/water solution at the composition where extensive water clustering is observed, i.e., $w_P = 0.9$, with water−water electrostatic interactions responsible for water−water hydrogen bonding turned off. As expected, turning off water−water electrostatic interactions results in the disappearance of water clusters and a dramatic increase in PEO−water hydrogen bonding as shown in Table 1. It is clear from Table 1 that elimination of water clustering at $w_P = 0.9$ leads to a dramatic slowing down of water rotational dynamics and a less dramatic slowing down of translational dynamics. Water residence times near EO and EO−H_W hydrogen bond residence times also increase as a result of elimination of water clustering.

TABLE 1: Dynamic Properties of Water in $w_P = 0.9$ PEO/Water Solutions with and without Water−Water Electrostatic Interactions

property\system	water−water electrostatic turned on	water−water electrostatic turned off
fraction of water hydrogen bonded to PEO (%)	80.1	99.1
τ_1(HH) (ps)	13.2	19
τ_2(HH) (ps)	23.0	76
τ_1(HH)/τ_2(HH)	0.57	0.25
$\tau_1(\mu)$ (ps)	61.8	142
$\tau_2(\mu)$ (ps)	19.9	59
$\tau_1(\mu)/\tau_2(\mu)$	3.1	2.4
D_W (10^{-10} m^2/s)	3.4	2.4
τ_1(EO−H_W) residence time (ps)	67.5	287
τ_2(EO−H_W) residence time (ps)	3.7	4.11

Hence, it appears that water interactions with PEO are primarily responsible for slowing down water dynamics in PEO/water solutions and that formation of water clusters in relatively concentrated solutions moderates these effects by reducing the number of PEO/water interactions.

VIII. Conclusions

MD simulations of PEO/water solutions have shown that water translational motion can be described as being due to a combination of free water (water not involved with PEO hydration) that exhibits bulklike water dynamics and bound (hydrating water) whose motion is strongly correlated with that of the PEO molecule. Water−water and water−ether oxygen hydrogen bond lifetimes, rotational and translational characteristic relaxation times showed an approximately exponential increase with polymer weight fraction increase.

The predicted slowing of water rotational relaxation with increasing PEO concentrations was in good agreement with NMR studies. Rotational motion around the μ axis of waters bound to PEO was significantly less perturbed than for either rotation of this vector (μ) or translational motion. Water rotation relaxation exhibited increasingly anisotropic dynamics with increasing polymer concentration, with water rotation in the plane perpendicular to μ being much faster than the rotation of the μ vector at high PEO concentrations in PEO/water solutions with the rotation of the μ vector being isotropic for all concentrations. A decrease of water rotational and translational diffusion with increasing PEO concentrations correlates well with the increasing water caging with PEO concentration increase. The characteristic size of the cages from analysis of the intermediate incoherent structure factor of water coincides nicely with the closest distance of PEO oxygen atoms from different chains. The subdiffusive behavior of water molecules caused by caging is intimately related to subdiffusive motion of PEO oxygen atoms, which is the most pronounced in pure PEO and gradually disappears with dilution of PEO with water.

Finally, MD simulations without water−water electrostatic interactions at $w_P = 0.9$ lead to dramatically reduced water clustering, which allowed us to study the influence of water clusters on water and PEO dynamics. The elimination of water clustering leads to a slowing down of water rotational and translational dynamics as well as a significant increase of the EO−H_W hydrogen bond and water−EO residence times. This allowed us to conclude that water interactions with PEO are primarily responsible for slowing down water dynamics in PEO/water solutions and that formation of water clusters in relatively concentrated solutions moderates these effects by reducing the number of PEO/water interactions.

Acknowledgment. The authors are indebted to the National Science Foundation, Division of Materials Research, for support through NSF award DMR 0076306. An allocation of computer time from the center for the High Performance Computing at the University of Utah is gratefully acknowledged. We also would like to thank R. Boyd for helpful discussions.

References and Notes

(1) McPherson, A. *Methods Enzymol.* **1985**, *114*, 112.
(2) McPherson, A. *J. Cryst. Growth* **1991**, *110*, 1.
(3) Cudney, B.; Patel, S. *Acta Crystallogr.* **1994**, *D50*, 414.
(4) Harris, J. M. In *Poly(Ethylene Glycol) Chemistry: Biotechnical and Biomedical Applications*; Harris, J. M., Ed.; Plenum Press: New York, 1992; p 1.
(5) Andrade, J. D.; Hlady, V.; Jeon, S. I. *Polym. Mater.: Sci. Eng.* **1993**, *69*, 60.
(6) Asakura, S.; Oosawa, F. *J. Polym. Sci.* **1958**, *33*, 183.
(7) Poon, W. C. K.; Pirie, A. D.; Haw, M. D.; Pusey, P. N. *Physica A* **1997**, *235*, 110.
(8) Rex, S.; Zuckermann, M. J.; Lafleur, M.; Silvius, J. R. *Biophys. J.* **1998**, *75*, 2900.
(9) Evans, E.; Rawicz, W. *Phys. Rev. Lett.* **1997**, *79*, 2379.
(10) Albertsson, P. In *Aqueous Biphasic Separations*; Rogers R. D., Eiteman, M. A., Eds.; Plenum Press: New York, 1995; p 21.
(11) Smith, G. D.; Borodin, O.; Bedrov, D. *J. Comput. Chem.* Submitted for publication.
(12) Bedrov, D.; Borodin, O.; Smith, G. D. *J. Phys. Chem. B* **1998**, *102*, 5683.
(13) Bedrov, D.; Borodin, O.; Smith, G. D. *J. Phys. Chem. B* **1998**, *102*, 9565.
(14) Bedrov, D.; Smith, G. D. *J. Phys. Chem. B* **1999**, *103*, 3791.
(15) Bedrov, D.; Borodin, O.; Smith, G. D.; Trouw, F.; Mayne, C. *J. Phys. Chem. B* **2000**, *104*, 5151.
(16) Liu, H.; Müller-Plathe, F.; van Gunsteren, W. F. *J. Chem. Phys.* **1995**, *102*, 1722.
(17) Engkvist, O.; Åstrand, P.-O.; Karlström, G. *J. Phys. Chem.* **1996**, *100*, 6950.
(18) Williams, D. J.; Hall, K. B. *J. Phys. Chem.* **1996**, *100*, 8224.
(19) Tasaki, K. *J. Am. Chem. Soc.* **1996**, *118*, 8459.
(20) Engkvist, O.; Karlström, G. *J. Chem. Phys.* **1997**, *106*, 2411.
(21) Borodin, O.; Trouw, F.; Bedrov, D.; Smith, G. D. *J. Phys. Chem. B* **2002**, *106*, 5184.
(22) Borodin, O.; Bedrov, D.; Smith, G. D. *Macromolecules* **2001**, *34*, 5687.
(23) Smith, G. D.; Bedrov, D.; Borodin, O. *Phys. Rev. Lett*, **2000**, *85*, 5583.
(24) Borodin, O.; Trouw, F.; Smith, G. D.; Bedrov, D.; Douglas, R. Manuscript is in prepapation.
(25) Smith, G. D.; Jaffe, R. L.; Yoon, D. Y. *J. Phys. Chem.* **1993**, *97*, 12752.
(26) Jorgensen, W. L.; Chandrasekhar, J.; Madura, J. D.; Impey, R. W.; Klein, M. *J. Chem. Phys.* **1983**, *79*, 926.
(27) Allen, M. P.; Tildesley, D. J. *Computer Simulation of Liquids*; Oxford University Press: New York, 1987.
(28) Ryckaert, J. P.; Ciccotti, G.; Berendsen, H. J. C. *J. Comput. Phys.* **1977**, *23*, 327.
(29) Tuckerman, M.; Berne, B. J.; Martyna, G. J. *J. Chem. Phys.* **1992**, *97*, 1990.
(30) Martyna, G. J.; Tuckerman, M.; Tobias, D. J.; Klein, M. L. *Mol. Phys.* **1996**, *87*, 1117.
(31) Ambrosone, L.; D'Errico, G.; Sartorio, R.; Costantino, L. *J. Chem. Soc., Faraday Trans.* **1997**, *93*, 3961.
(32) Lüsse, S.; Arnold, K. *Macromolecules* **1996**, *29*, 4251.
(33) Factor 2.6 is equal to the product of two factors: $\tau_2^{HH}(T = 298\ K)/\tau_2^{HH}(T = 318\ K)$ equal for TIP4P water to 1.32 and a factor of 2 taking into account rotational dynamics of D_2O vs H_2O.
(34) van der Spoel, D.; van Maaren, P. J.; Berendsen, H. J. C. *J. Chem. Phys.* **1998**, *108*, 10220.
(35) Sciortino, F.; Gallo, P.; Tartaglia, P.; Chen, S.-H. *Phys. Rev. E* **1996**, *54*, 6331.
(36) Crupi, V.; Magazu, S.; Majolino, D.; Migliardo, P.; Wanderlingh, U.; Kagunya, W. W. *Physica B* **1998**, *241−243*, 979.
(37) Crupi, V.; Jannelli, M. P.; Magazù, S.; Maisano, G.; Majolina, D.; Migliardo, P.; Vasi, C. *Il Nuovo Cimento* **1994**, *16*, 809.
(38) de Gennes, P.-G. *Scaling Concepts in Polymer Physics*; Cornell University Press: Ithaca, NY, 1979.